



THE MODELLING OF ICE-STRUCTURE INTERACTION WITH COHESIVE ELEMENT METHOD: LIMITATIONS AND CHALLENGES

Sze Dai Pang ¹, Jin Zhang ¹, Leong Hien Poh ¹, Elliot Law ², Kim Thow Yap ³

¹Department of Civil & Environmental Engineering, National University of Singapore

²Engineering Design and Innovation Centre, National University of Singapore

³Keppel Offshore & Marine Technology Centre, Singapore

ABSTRACT

Ice sheet failure mechanism is highly complex and has multiple modes of failure (crushing, flexural failure, radial and circumferential cracking, spalling and creep) which can occur simultaneously in ice-structure interaction. The capability of the Cohesive Element Method (CEM) to simulate realistic ice fracture phenomenon makes it a promising numerical method which can be developed into a useful numerical tool for design of offshore structures subjected to ice actions.

In recent years, there has been greater interest and development of the CEM framework for ice-structure interactions (e.g. Gürtner *et al.*, 2009; Konuk *et al.*, 2009; Gürtner *et al.*, 2010; Hilding *et al.*, 2011; Liu and Wu, 2012). Most of the efforts have been dedicated to the demonstration of ice fracture and crushing in the event of an ice-structure interaction. However, there are a number of limitations and challenges which have not been fully addressed and these include the use of a uniform mesh with hexahedral elements, lack of convergence with mesh refinement, large variation in the properties of the cohesive elements, as well as assumptions made in model implementation.

In this paper, a comprehensive survey of the literature on CEM applied to ice-structure interaction is presented. The advancement of the CEM till date is discussed and its limitations are exemplified with simulations carried out in this study. Approaches to overcome some of these challenges are proposed and supported by simulation results.

INTRODUCTION

Large scale experimental testing of in-situ sea ice is highly challenging and expensive. This limitation can be overcome by numerical tests with realistic modelling. In the modelling of ice-structure interaction with features that span over orders of magnitude from the small ice fragments to the semi-infinite ice sheets, this will entail computationally intensive simulations. However, with advancing computation and development of numerical methods, it becomes more feasible to use numerical tests to predict the response of ice-structure interactions.

The failure mechanism of sheet ice can be highly complex and involves multiple modes of failure (crushing, flexural failure, radial and circumferential cracking, spalling and creep) which can occur simultaneously in ice-structure interaction. In order to simulate the fracturing

of ice, the different numerical approaches range from the basic finite element method (FEM) approach which incorporates element erosion, to the discrete element method (DEM) which incorporates cohesive contact between the particles and the extended finite element method (XFEM) which promises mesh free simulation of arbitrary cracks (Lu *et al.*, 2012b). Alternative hybrid methods include the Particle-In-Cell method (PIC) in which the particles are advected in a Lagrangian manner while their momentum equations are solved over an Eulerian grid (Barker and Sayed, 2013).

The drawback of conventional FEM with element erosion is the violation of conservation laws as the removal of elements also removes mass and energy from the system. Furthermore, the absence of ice fragments does not allow for the interaction between the ice rubbles and the ice sheet/structure to be explicitly simulated. While DEM seems to be mesh-free, the tracking of individual particles requires extreme computational efforts. In addition, cohesive contact properties between the particles need to be artificially calibrated. XFEM allows for the crack propagation to be independent of mesh and conserves mass. Similar to traditional FEM, it is unable to simulate the rubbing effect of crushed ice fragments. Although PIC has been used to study broken ice cover forces on structures and build up effect, the disintegration of ice cover into ice floes does not explicitly follow fracture theory. In the simulation of ice crushing when it interacts with a structure, the process is governed by fracture and plasticity, which will currently favour the FEM over the other alternative approaches.

The cohesive element method (CEM) is a blend between FEM and DEM which improves on their individual drawbacks. Cohesive elements with vanishing thickness are inserted between the bulk elements. The constitutive relations for the volume elements and the cohesive elements are different; the volume element follows the properties of the bulk material while fractures are modelled by the cohesive elements with its separation following the traction-separation law. Conservation laws are satisfied as only near-zero thickness cohesive elements are removed. Multiple fractures can be simulated by prescribing cohesive elements at all potential crack surfaces. However, the propagation of the cracks becomes dependent on both mesh size and geometry, leading to large variations in the specifications of cohesive element properties by researchers. The challenges in implementing the CEM and approaches to overcome them will be discussed in subsequent sections.

COHESIVE ELEMENT METHOD

The classical linear elastic fracture mechanics (LEFM) theory is strictly applicable when the size of the fracture process zone (FPZ) is small compared to the relevant dimensions of the specimen. In many quasi-brittle materials where the FPZ cannot be lumped into the crack tip, the FPZ can be described by simplified model of a fictitious crack that transfers stress from one crack face to the other, such as the cohesive zone model (CZM). The FPZ accounts for the nonlinear behaviour of the material ahead of the tip of a pre-existent crack and these models made it possible to relieve the crack tip singularity.

The cohesive zone model (CZM) was pioneered by Barenblatt (1959, 1962) and Dugdale (1960) for applications in the fracture of brittle and ductile materials respectively. Crack initiation and propagation in quasi-brittle concrete was implemented in the finite element framework by Hillerborg *et al.* (1976) with the use of CZM by adopting fracture mechanics theories such as the stress intensity factor and energy balance approach. The implementation of the CZM into numerical analysis has been commonly referred to as the Cohesive Element Method (CEM) which entails the insertion of cohesive inter-elements between bulk elements

in the conventional finite element mesh. This is achieved by duplicating the nodes along all internal mesh boundaries as shown in Figure 1.

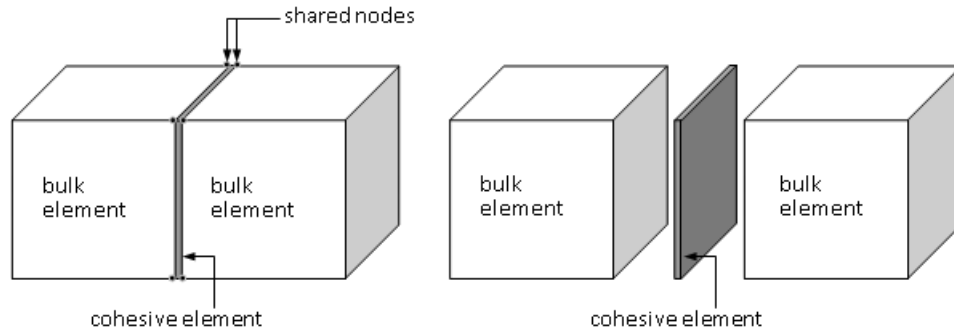


Figure 1. Insertion of cohesive element between bulk elements.

These cohesive elements follow a traction-separation law which describes the material separation process and provides a relation between crack surface traction and crack surface opening displacement. Upon reaching the separation limit, the cohesive elements fail and are removed, thus explicitly simulating the fracture process zone (FPZ) which is confined along the finite element boundaries. The cohesive element does not represent any physical material but describes the cohesive forces when fracture occurs. The stresses are finite everywhere in the vicinity of the crack tip and there is no need to solve for stress-singularities. Thus, this model is based on the robust mathematical framework of conventional FEM and relies on the cohesive elements for crack propagation. The cohesive elements have negligible mass and volume as compared to the bulk elements and hence, the erosion of the cohesive elements does not violate the conservation law, as opposed to bulk element erosion method in traditional FEM.

IMPLEMENTATION OF CEM IN ICE-STRUCTURE INTERACTION

CEM methodology was adopted by Gürtner *et al.* (2009) in the modelling of ice-structure interaction and research interest in this area has gained momentum in the latter years (Hilding *et al.*, 2011). The development of a basic CEM model in LS-DYNA can be referenced from a few main papers: "Numerical modelling of a full scale ice event" (Gürtner *et al.*, 2010), "Simulation of ice action loads on offshore structures" (Hilding *et al.*, 2011) and "Numerical simulation of the ice-structure interaction in LS-DYNA" (Daiyan and Sand, 2011). In these three papers, the ice-structure interaction is that of a 40 x 40 x 0.69 m ice-sheet drifting at 0.15 m/s and impacting the Norströmsgrund lighthouse structure which is of a cylindrical form with diameter of 7.2 m. The Norströmsgrund lighthouse is located in the Gulf of Bothnia near Luleå, Sweden, and full-scale measurements of ice forces have been carried out during the winters of 1999 to 2003 (Kärnä and Jochmann, 2003). The physical measurements of structure loading as shown in Figure 2 can be referenced from Hilding *et al.* (2012). Figure 2(a) shows the accumulation of ice fragments during a continuous crushing event and Figure 2(b) shows the corresponding measured forces exerted on the lighthouse.

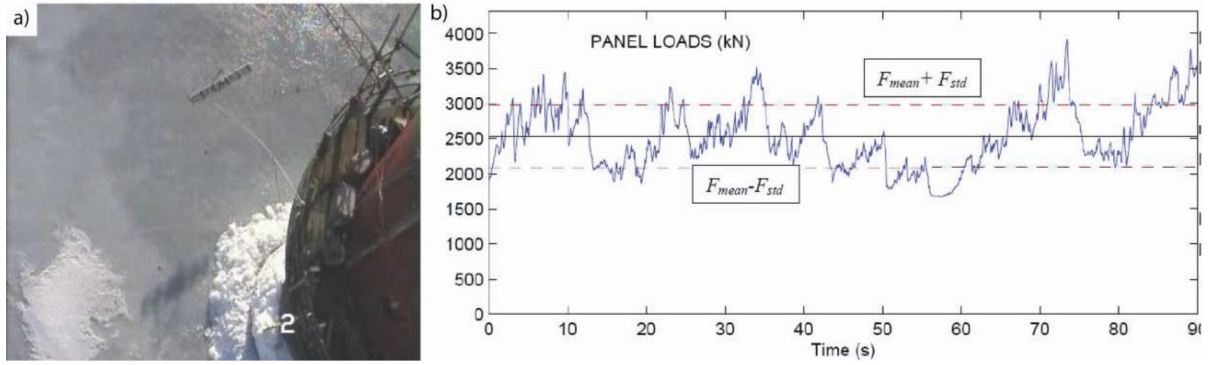


Figure 2. Physical measurements and ice failure at Norströmsgrund lighthouse (Hilding *et al.*, 2012).

In this study, the interaction zone is assumed to be 20 x 20 m with bulk element size of about 0.2 x 0.2 x 0.13 m to reduce the computation time. Cohesive elements with vanishing thickness are inserted between the bulk elements as described in the preceding section. Figure 3 illustrates how the cohesive elements are used to connect the bulk elements to each other. The material properties of the bulk elements and cohesive elements are referenced from Gürtner *et al.* (2010) and Hilding *et al.* (2012) and shown in Table 1. Figure 4 shows the typical full model at initial timestep where the ice sheet advances towards the 7.2 m diameter cylinder at a constant velocity of 0.15 m/s.

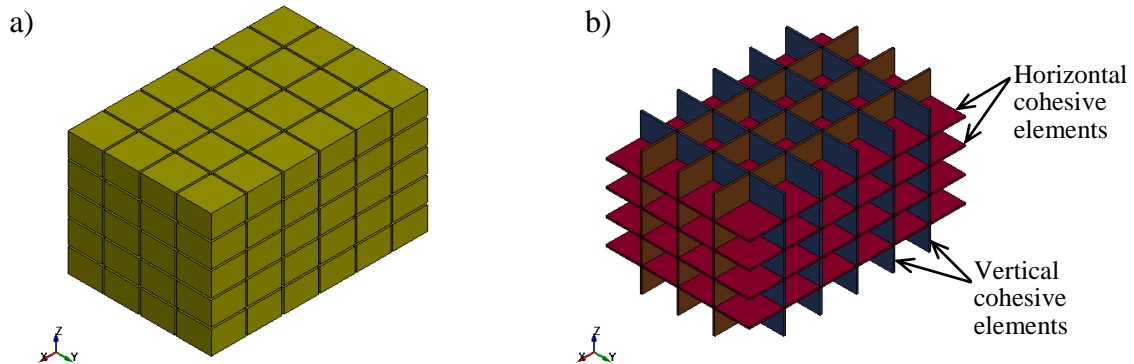
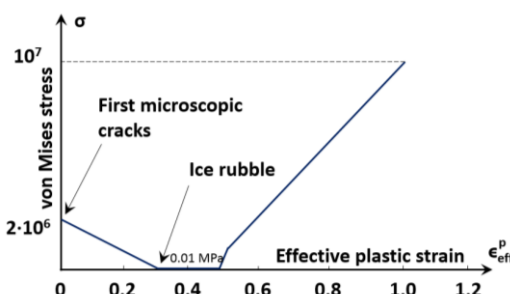
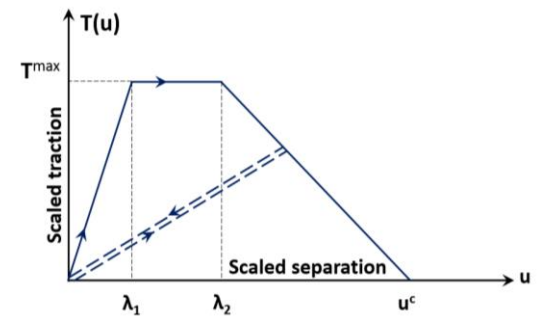


Figure 3. The ice sheet is modelled with a combination of a) bulk elements, and b) cohesive elements.

Table 1. Material properties (Gürtner *et al.*, 2010; Hilding *et al.*, 2012).

Bulk elements	Cohesive elements
 <p>von Mises stress σ</p> <p>Effective plastic strain ϵ_{eff}^p</p> <p>First microscopic cracks</p> <p>Ice rubble</p> <p>0.01 MPa</p> <p>2·10⁶</p> <p>10⁷</p> <p>0 0.2 0.4 0.6 0.8 1.0 1.2</p>	 <p>$T(u)$</p> <p>Scaled traction</p> <p>T_{max}</p> <p>λ_1 λ_2 u^c</p> <p>Scaled separation u</p>
<p>$E = 5 \text{ GPa}$</p> <p>$\rho = 910 \text{ kg/m}^3$</p> <p>$\nu = 0.3$</p> <p>$\sigma_y = 2.0 \text{ MPa}$</p>	<p>$G_{IC} = 5200 \text{ J/m}^2$</p> <p>$G_{IIC} = 5200 \text{ J/m}^2$</p> <p>$\lambda_1 = 0.02$ (vert. & hori.)</p> <p>$\lambda_2 = 0.55$ (vert.)</p> <p>$\lambda_2 = 0.45$ (hori.)</p> <p>$T_{max, \text{ tensile}} = 1.0 \text{ MPa}$ (vert.)</p> <p>$T_{max, \text{ shear}} = 1.0 \text{ MPa}$ (vert.)</p> <p>$T_{max, \text{ tensile}} = 1.1 \text{ MPa}$ (hori.)</p> <p>$T_{max, \text{ shear}} = 1.1 \text{ MPa}$ (hori.)</p>

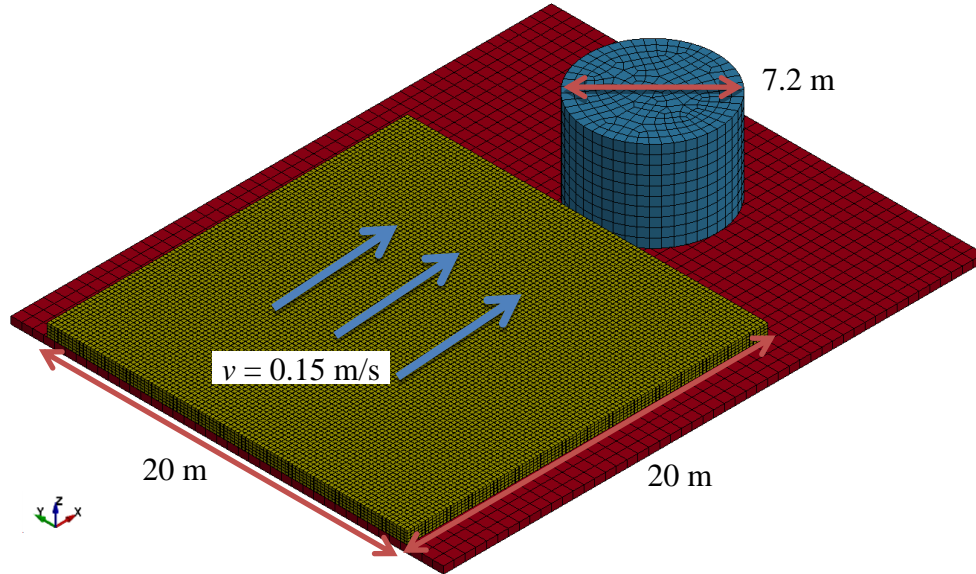


Figure 4. Typical full model at initial timestep.

CURRENT CHALLENGES

Limitations of a Uniform Mesh with Hexahedral Elements

In a uniform mesh with hexahedral elements discretized in the global x , y , z axis as illustrated in Figure 4, the cracks can only propagate vertically or laterally. Attempts were made to model the anisotropic behaviour in columnar ice by specifying different properties for the cohesive zone elements in the vertical and horizontal planes (Gürtner *et al.*, 2009; Konuk *et al.*, 2009; Gürtner *et al.*, 2010; Hilding *et al.*, 2011; Liu and Wu, 2012). While the use of a uniform hexahedral mesh might be the most convenient approach to model fragmentation of a large number of particles using cohesive elements, it constrains the potential cracks to propagate only along these orthogonal planes as shown in Figure 5. To reduce the constraints on the possible fracture paths, Lu *et al.* (2012a) had tried to study a crossed triangular mesh pattern which would allow for both diagonal and orthogonal cracks to form. However, it was reported that the mean load increased with mesh refinement and convergence was yet to be

achieved. Furthermore, it should be noted that the crossed triangular mesh pattern studied by Lu *et al.* makes use of triangular block elements which will facilitate diagonal cracking in the horizontal plane but discretization along the vertical depth remains the same as the hexahedral mesh which only allows for cracks to propagate in the x - y plane. In comparison, a fully tetrahedral mesh which would allow for diagonal crack paths in both vertical and horizontal planes will be explored in the subsequent section of this paper.

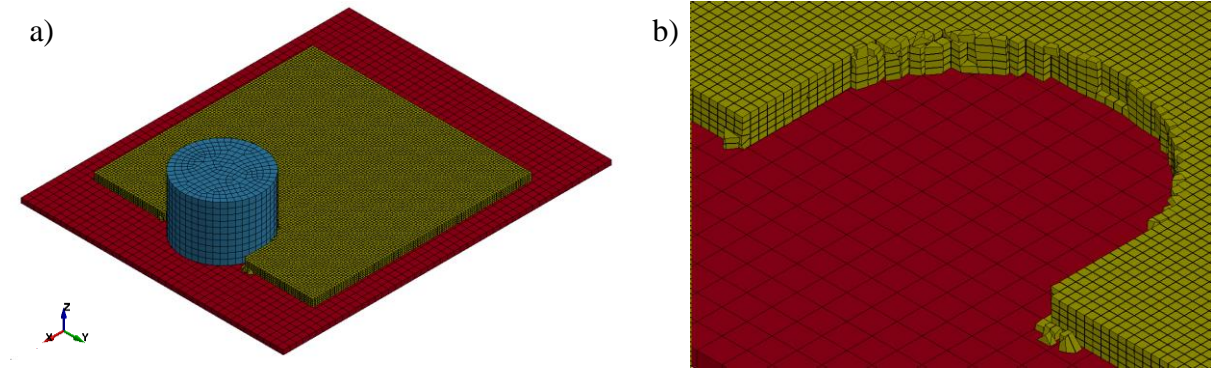


Figure 5. a) Rubbled ice in front of lighthouse is removed for illustration, and b) Close up of surface interaction.

Lack of Convergence with Mesh Refinement

The placing of cohesive elements on every possible interface is by far the most developed methodology to handle many simultaneous cracks such as fragmentation problems. In order for the numerically simulated crack path to follow closely to the true crack path, a sufficiently fine mesh could be used to enrich the set of potential paths that the crack can follow. However, a convergence proof for the cohesive finite elements as the mesh size tends to 0 is still lacking in literature (Papoulia *et al.*, 2003).

Hilding *et al.* (2012) suggests a homogenization approach in an attempt to capture the macroscopic effect of ice crushing without the need to model all the small cracks. Using a representative volume element, the amount of internal cracks is assumed to be proportional to the amount of deformation. The average effects of the cracks are then expressed on the macroscopic level by subjecting the bulk elements to softening following a yield curve as shown in Table 1 above. This material model is size independent since the energy for this material model scales with Length^3 yet physically captures the plastic energy (which scales with Length^3) and the fracture energy (which scales with Length^2). The purpose of the bulk and cohesive elements are not clearly differentiated here as both the bulk and cohesive elements account for fracture. Nevertheless, this material model is considered as a simulation case for comparison and the results are presented below.

The effects of mesh refinement are studied by simulating the ice sheet using three different mesh sizes while keeping all other parameters constant. Figure 6 shows the simulation results at time of 30 seconds after initial impact. The ice sheet in Case 1 is meshed using element size of $0.2 \times 0.2 \times 0.138$ m, while Case 2 uses element size of $0.4 \times 0.4 \times 0.138$ m and Case 3 uses element size of $0.8 \times 0.8 \times 0.138$ m. The vertical height of the element is maintained throughout so that there are 5 elements across the thickness of the ice sheet. The computational times for the various models are as follows: Case 1 ~ 152 hours with 8 CPUs, Case 2 ~ 36 hours with 8 CPUs, Case 3 ~ 18 hours with 4 CPUs.

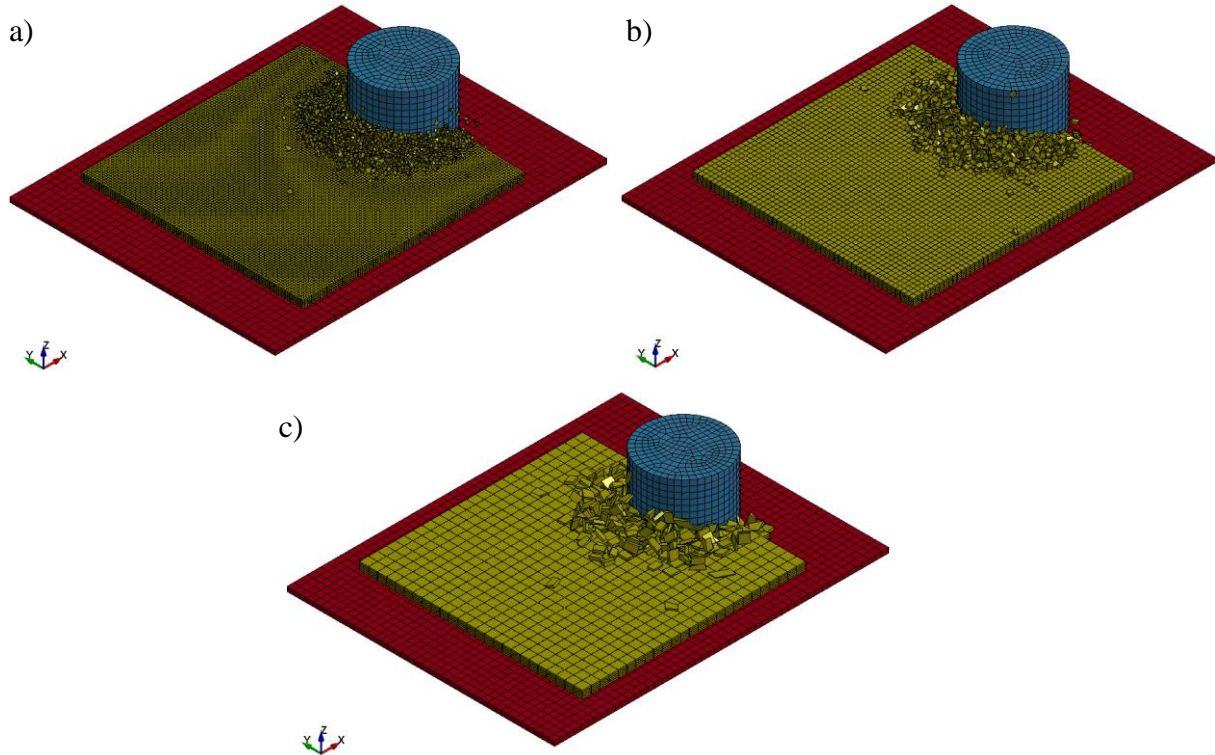


Figure 6. Ice-structure interaction at 30 seconds after initial impact for a) Case 1: Fine mesh, b) Case 2: Medium mesh, and c) Case 3: Coarse mesh.

For a constant driving velocity of 0.15 m/s for the ice sheet, the full width of the structure would be interacting with the ice sheet after 24 s. The total horizontal force experienced by the structure after 24 s is output and shown in Figure 7. The average force and the standard deviation for all the three cases are tabulated in Table 2 for comparison. Case 3 with the coarse mesh shows the lowest average force of 1.61 MN but with the largest standard deviation of 0.876 MN. Case 2 with the medium mesh shows an average force of 2.22 MN with a smaller fluctuation of 0.487 MN. Case 1 with the finest mesh shows an average force of 3.49 MN with a standard deviation of 0.119 MN. Clearly, the average force increases with refinement in mesh size and there is no convergence in the predicted forces for the different mesh sizes. It should be noted that the dispersion of the force, characterized by the coefficient of variation of the force, is highly dependent on the fragmentation process (fragment size, rate of clearing of fragments from crushed zone); the value varies from 0.119 for the fine mesh to 0.544 for the coarse mesh, while the value from the physical measurements is 0.18.

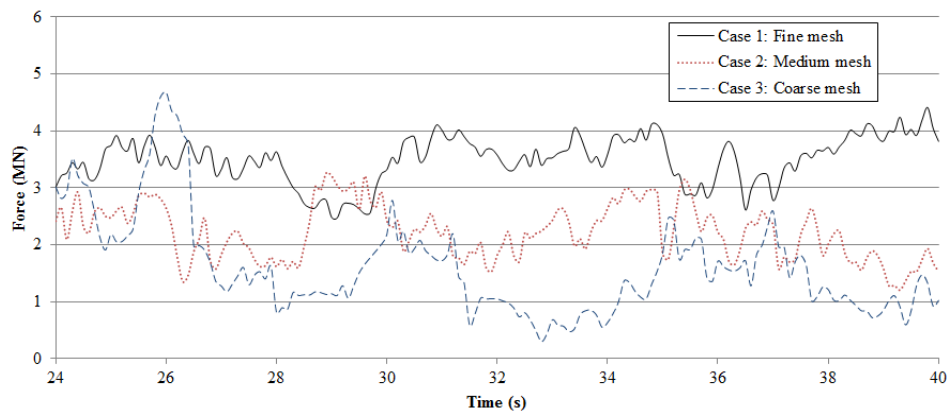


Figure 7. Ice-structure interaction forces as the ice rubbles against the lighthouse.

Table 2. Prediction of average force using different mesh sizes

	Case 1: Fine mesh (MN)	Case 2: Medium mesh (MN)	Case 3: Coarse mesh (MN)
F_{mean}	3.49	2.22	1.61
F_{std}	0.415	0.487	0.876
$CoV = F_{\text{std}} / F_{\text{mean}}$	0.119	0.219	0.544

Figure 8 shows the comparison of the internal energy of bulk elements for the three different mesh sizes. The rate of bulk energy dissipation increases with a coarsening in mesh size, which shows the mesh dependence of the energy dissipation. As the elements get larger, the fragments are harder to be freed from the crushing zone which resulted in a higher rate of dissipation of bulk energy. The same mesh dependency issue is observed for the rate of cohesive energy dissipation. Both the bulk and cohesive energies show strong dependence on mesh size which has not been resolved.

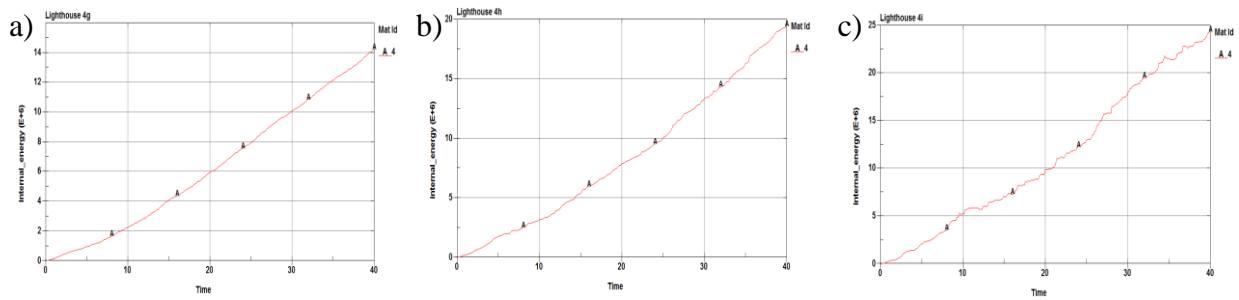


Figure 8. Internal energy of bulk elements for models using a) Case 1: Fine mesh, b) Case 2: Medium mesh, and c) Case 3: Coarse mesh.

The three cases above have been based on the same constitutive model and parameters for the bulk elements and the cohesive elements despite the change in mesh size. It is clearly shown that both the yield curve for the bulk elements and the traction separation law for the cohesive elements are dependent on mesh size and hence should be scaled adequately to eliminate mesh dependency.

Large Variation in the Properties of the Cohesive Elements

The traction separation law that describes the behaviour of the cohesive elements under tensile and shear stresses has been shown above in Table 1. For a linear softening model, the traction separation law can be defined by the parameters E , T_{max} and G_C . For a plastic softening model, there is a need to define two non-dimensional parameters δ_1 and δ_2 which characterize the plastic region. The stiffness of the cohesive elements, E , is commonly treated as a penalty parameter to ensure that the overall stiffness of the ice specimen is not reduced much by the presence of the cohesive elements with finite stiffness. The cohesive strength, T_{max} , is sometimes treated as a penalty parameter if the cohesive length is sufficiently small such that only the fracture energy matters. Table 3 illustrates the large variations in the specifications of cohesive element properties assumed by the respective authors during model implementation.

It can be observed that the cohesive strength differs by more than one order of magnitude, ranging from 0.065 MPa to 1.0 MPa. The fracture energy that was determined experimentally in the lab ranges around 1–2 J/m² (Timco and Weeks, 2010) and it differs by more than one order of magnitude as compared to the values shown in Table 3, which ranges around

52–5200 J/m². These values are often adopted to match the load predictions measured in the field. Even though Dempsey *et al.* (2012) reported values between 23–47 J/m², the much larger value is believed to be due to the slower rate of loading in the field testing of large specimens which leads to larger creep.

Table 3. Bulk and cohesive element properties.

Paper Title / Authors / Year	Bulk element	Bulk element properties	Traction-separation law	Cohesive element properties
Numerical simulation of ice action to a lighthouse / <i>Gurner, Bjerkås, Khnlein, Jochmann and Konuk</i> / 2009	8-nodes brick 0.17x0.4x0.4 m	von Mises yield $E = 1000 \text{ GPa}$ $\rho = 910 \text{ kg/m}^3$ $\nu = 0.3$ $\sigma_y = 0.0007 \text{ MPa}$	Plastic softening	$G_{IC} = 20 \text{ J/m}^2$ (vert.) $G_{IIC} = 28 \text{ J/m}^2$ (vert.) $G_{IC} = 52 \text{ J/m}^2$ (hori.) $G_{IIC} = 52 \text{ J/m}^2$ (hori.) $\lambda_1 = 0.08$ (vert.) $\lambda_2 = 0.45$ (vert.) $\lambda_1 = 0.10$ (hori.) $\lambda_2 = 0.55$ (hori.)
Study of Dynamic Ice and Cylindrical Structure Interaction by the Cohesive Element Method / <i>Konuk, Gurner and Yu</i> / 2009	8-nodes brick	von Mises yield $E = 5.0 \text{ GPa}$ $\rho = 910 \text{ kg/m}^3$ $\sigma_y = 2.0 \text{ MPa}$	Linear softening	$T_{\max} = 0.5 \text{ MPa}$ (vert.) $T_{\max} = 0.6 \text{ MPa}$ (hori.) $E_{//} = 50 \text{ GPa/m}$ (vert.) $E_{\perp} = 5 \text{ GPa/m}$ (vert.) $E_{//} = 50 \text{ GPa/m}$ (hori.) $E_{\perp} = 5 \text{ GPa/m}$ (hori.)
Numerical modelling of a full scale ice event / <i>Gurner, Bjerkås, Forsberg and Hilding</i> / 2010	8-nodes brick 0.13x0.2x0.2 m	von Mises yield $E = 5.0 \text{ GPa}$ $\nu = 0.3$ $\sigma_y = 1.5 \text{ MPa}$	Plastic softening	$T_{\max} = 1.0 \text{ MPa}$ (vert.) $T_{\max} = 1.1 \text{ MPa}$ (hori.) $G_C = 5200 \text{ J/m}^2$ $\lambda_1 = 0.02$ $\lambda_2 = 0.55$ (vert.) $\lambda_2 = 0.45$ (hori.) $u^c = 6.8 \text{ mm}$ (vert.) $u^c = 7.1 \text{ mm}$ (hori.)
Simulation of ice action loads on offshore structures / <i>Hilding, Forsberg and Gurner</i> / 2011	8-nodes brick 0.13x0.2x0.2 m	von Mises yield $E = 5.0 \text{ GPa}$ $\rho = 910 \text{ kg/m}^3$ $\nu = 0.3$ $\sigma_y = 2.0 \text{ MPa}$	Plastic softening	$T_{\max} = 1.0 \text{ MPa}$ (vert.) $T_{\max} = 1.1 \text{ MPa}$ (hori.) $G_C = 5200 \text{ J/m}^2$
Numerical simulation for ice-truss offshore structure interactions with cohesive zone model / <i>Liu and Wu</i> / 2012	8-nodes brick	von Mises yield $E = 5.0 \text{ GPa}$ $\rho = 910 \text{ kg/m}^3$ $\sigma_y = 2.0 \text{ MPa}$	Plastic softening	$T_{\max} = 0.065 \text{ MPa}$ (vert.) $T_{\max} = 0.071 \text{ MPa}$ (hori.) $G_{IC} = 20 \text{ J/m}^2$ (vert.) $G_{IIC} = 28 \text{ J/m}^2$ (vert.) $G_{IC} = 52 \text{ J/m}^2$ (hori.) $G_{IIC} = 52 \text{ J/m}^2$ (hori.) $u^c = 0.095 \text{ mm}$ (vert.) $u^c = 0.200 \text{ mm}$ (hori.)

PROPOSED SOLUTIONS TO CHALLENGES

Properties of the Cohesive Elements

The formulation of interface elements with non-zero thickness requires a finite stiffness prior to the onset of cracking, thus giving rise to deformations in the interface before crack initiation. Often, these unwanted deformations are largely suppressed by choosing a very high arbitrary stiffness in the interface for the pre-cracking phase. Depending on the chosen spatial integration scheme, this high dummy stiffness can lead to numerical instability for explicit time stepping schemes and spurious traction oscillations in the pre-cracking phase, which may cause erroneous load predictions. While the results presented in this paper are based on interface elements with finite thickness, numerical studies are also being carried out with the use of zero thickness interface elements and the results will be presented in the conference. The necessity of using zero thickness interface elements in this study is described in greater detail in the next section.

In the quasi-static loading, the specimen is in static equilibrium during the loading process and cracks will initiate at the weaker planes which will then lead to subsequent failure along these weak planes. For anisotropic materials, the weaker planes will potentially govern the failure and would need to be explicitly accounted for in order to simulate the failures along the weaker planes. At faster rates of loading, the stress waves could potentially exceed the strength and energy limits of the material with no regards to the strong or weak planes, leading to fragmentation of a large number of small particles, which was commonly observed for the crushing of ice during ice-structure interaction. For such behaviour, it suffices to use effective traction and separation parameters to take into account the anisotropy and mode-mixity without the need to model these effects explicitly. In other words, the complex fracture mechanism could be lumped into effective properties that account for these effects. If the size of the elements is representative of the size of the fragments, the effective properties of the cohesive elements represent the average energy of all physical cracks (regardless of the mode of fracture) at the meso-level.

Since the fragmentation of ice will necessitate complete separation of the cohesive elements and complete dissipation of the fracture energy, the fracture energy will be one important parameter that needs to be estimated as accurately as possible. Even though the yield strength of the elements does not vary much (15–20MPa), the bulk energy dissipation is dependent on the fracture of the surrounding cohesive elements and hence indirectly dependent on the cohesive element properties. A sensitivity study on the cohesive strength and fracture energy should be carried out to ascertain the importance of these two parameters in ice-crushing failure during ice-structure interaction. Scaling laws should be subsequently developed such that the physical properties of the ice fragments can be scaled up correctly to the larger mesh sizes used in simulations, thus allowing for more efficient simulations with the cohesive element method.

Resolving Mesh Dependency

The mesh dependency with the use of CEM is an outstanding problem that has yet to be resolved. One approach for addressing mesh dependency of crack propagation is to employ very highly refined meshes (Arias *et al.*, 2007). However, mesh refinement increases cohesive energy dissipation due to increased surface area to volume ratio. On the other hand, bulk energy dissipation decreases with mesh refinement due to easier fragmentation of ice, leading to a lower accumulation of the bulk energy as shown in Figure 8. The properties of the cohesive and bulk elements should be properly scaled in tandem to eliminate mesh

dependency, thus allowing for larger elements to be adopted for more efficient computations on ice-structure interaction.

The limitations of a structured mesh with hexahedral elements have been described in the earlier part of this paper. It is generally agreed that an unstructured mesh produces more realistic fracture results (Needleman, 1990; Molinari *et al.*, 2007). Lu *et al.* (2012a) tried to improve upon the currently popular hexahedral mesh by proposing a crossed triangular mesh pattern which allows diagonal crack movement in-plane but restricts vertical movement orthogonally. To further facilitate the formation and propagation of cracks of shear cracks in- and out-of-plane of the ice sheet, the ice sheet can be discretized into tetrahedral elements shown in Figure 9(b). The nodes of the tetrahedral elements are also randomly perturbed as shown in Figure 9(c) to study the effects of irregular tetrahedral mesh and its associated random crack planes. The effect of the inclusion of the potential diagonal crack planes on the force-time and energy-time histories will be compared with the finite element model with hexagonal mesh to highlight the differences. The ice sheet used here for comparison of the different element types is smaller than the one described earlier to reduce the time for computation.

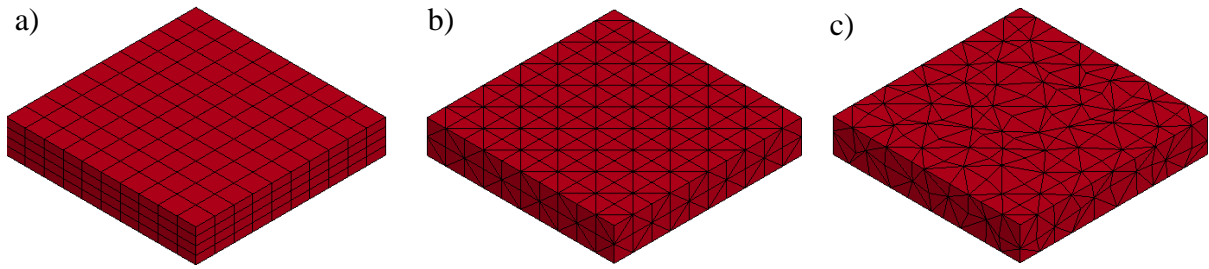


Figure 9: Discretization of ice sheet with a) uniform hexahedra, b) uniform tetrahedra, and c) tetrahedra with perturbed nodes.

Table 10 shows the force-time histories on the structure for the different element types. The lowest peak force is registered for the model with the uniform hexahedral mesh. This arises from the very large negative sliding energy and hourglass energy that accumulate rapidly upon contact between the ice and structure, leading to the propagation of an unrealistically large energy that lowered the force. When the tetrahedral elements are used, the force-time histories are more comparable even though a higher peak force is registered for the uniform tetrahedral mesh. The perturbation of the nodes further relieves the artificial constraints present in the crack planes that lie in the global x - y , y - z and x - z planes. The difference is more obvious if we compare the internal energies of the bulk elements as shown in Figure 11. The "locking" of the bulk elements due to the constraint of the crack planes in the global principal planes leads to an accumulation of internal energy for the uniform tetrahedral mesh.

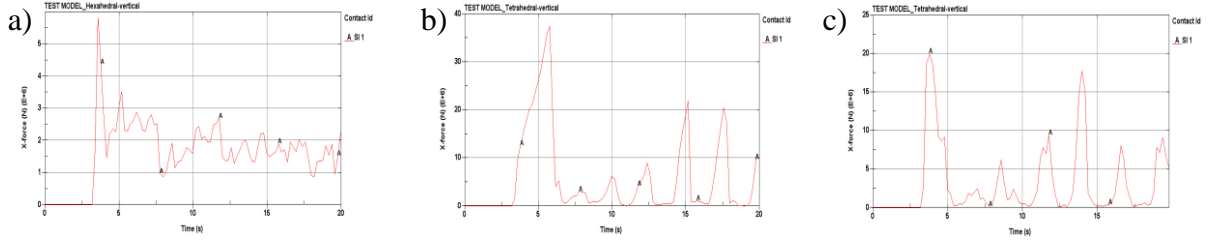


Figure 10: Force-time histories of ice sheet with a) uniform hexahedra, b) uniform tetrahedra, and c) tetrahedra with perturbed nodes.

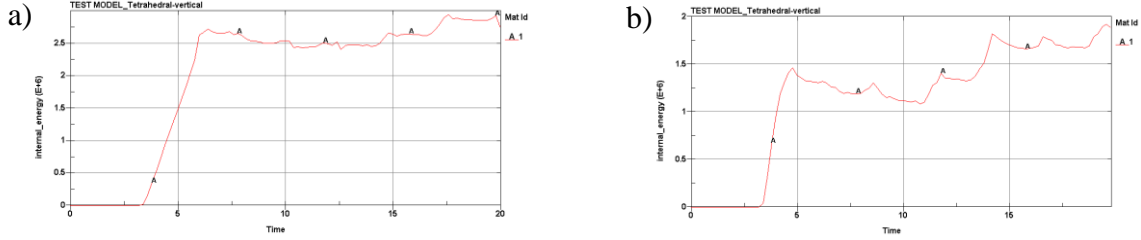


Figure 11: Internal energy-time histories for ice sheet with a) uniform tetrahedra, and b) tetrahedra with perturbed nodes.

Finally, a fully random tetrahedral mesh using Delaunay triangulation is currently being explored. The results for the comparison of all the different element types and their degree of randomness will be discussed at the conference.

CONCLUSION

CEM can explicitly simulate full scale simulations of ice sheets undergoing continuous crushing without violating the conservations laws. The structure becomes softened with increasing cohesive element density and hence a scaling law needs to be proposed for the cohesive element properties such that they correspond to the different mesh sizes. Arbitrary input of material properties need to be validated with experimental data, in particular full-scale ice-structure interaction data would be preferred. The prevalent choice of hexahedral mesh is simple to implement but limits crack propagation to orthogonal paths. By introducing a tetrahedral mesh, crack propagation can possibly be simulated more realistically due to available diagonal paths. A more ideal discretization approach would be a random tetrahedral mesh using Delaunay triangulation which allows for more physical representation of ice fragments with random sizes. Finally, properly scaled bulk and contact properties can potentially improve the convergence of the simulation results and are currently being studied in the research group.

ACKNOWLEDGEMENT

The authors thank the National Research Foundation of Singapore, Keppel Corporation and the National University of Singapore for supporting this work done in the Keppel-NUS Corporate Laboratory. The conclusions put forward reflect the views of the authors alone, and not necessarily those of the institutions within the Corporate Laboratory.

The authors thank Arne Gürtner for his kind comments.

REFERENCES

- Arias, I., Knap, J., Chalivendra, V.B., Hong, S., Ortiz, M. and Rosakis, A.J. (2007). Modeling and experimental validation of dynamic fracture events along weak planes. *Computer Methods in Applied Mechanics and Engineering*, Vol. 196, pp. 3833–3840.
- Barenblatt, G.I. (1959). The formation of equilibrium cracks during brittle fracture. General ideas and hypotheses. Axially-symmetric cracks. *Journal of Applied Mathematics and Mechanics*, Vol. 23, pp. 622–636.
- Barenblatt, G.I. (1962). The mathematical theory of equilibrium cracks in brittle fracture. *Advances in Applied Mechanics*, Academic Press, New York, pp. 55–129.
- Barker, A. and Sayed, M. (2013). Multi-Leg Structures in Ice – Examining Global Loading Uncertainties. *22nd International Conference on Port and Ocean Engineering under Arctic Conditions*, Espoo, Finland.
- Daiyan, H. and Sand, B. (2011). Numerical simulation of the ice –structure interaction in LS-DYNA. *8th European LS-DYNA Users Conference*, Strasbourg, France.
- Dempsey, J.P., Xie, Y., Adamson, R.M. and Farmer, D.M. (2012). Fracture of a ridged multi-year Arctic sea ice floe. *Cold Regions Science and Technology*, Vol. 76–77, pp. 63–68.
- Dugdale, D.S. (1960). Yielding of steel sheets containing slits. *Journal of the Mechanics and Physics of Solids*, Vol. 8, pp. 100–104.
- Gürtner, A., Bjerikås, M., Kühnlein, W., Jochmann, P. and Konuk, I. (2009). Numerical Simulation of Ice Action to a Lighthouse. *ASME 2009 28th International Conference on Ocean, Offshore and Arctic Engineering*, Honolulu, Hawaii, USA.
- Gürtner, A., Bjerikås, M., Forsberg, J. and Hilding, D. (2010). Numerical Modelling of a Full Scale Ice Event. *20th IAHR International Symposium on Ice*, Lahti, Finland.
- Hilding, D., Forsberg, J. and Gürtner, A. (2011). Simulations of Ice Action Loads on Offshore Structures. *8th European LS-DYNA Users Conference*, Strasbourg, France.
- Hilding, D., Forsberg, J. and Gürtner, A. (2012). Simulations of Loads from Drifting Ice Sheets on Offshore Structures. *12th International LS-DYNA Users Conference*, Detroit, USA.
- Hillerborg, A., Modeer, M., and Petersson, P.E. (1976). Analysis of crack formation and crack growth in concrete by means of fracture mechanics and finite elements. *Cement and Concrete Research*, Vol. 6, pp. 773–782.
- Kärnä, T. and Jochmann, P. (2003). Field Observations on Ice Failure Modes. *Proceedings of the 17th International Conference on Port and Ocean Engineering under Arctic Conditions*, POAC'03, Vol. 2, pp. 839–848. Trondheim, Norway.
- Konuk, I., Gürtner, A. and Yu, S. (2009). A Cohesive Element Framework for Dynamic Ice-Structure Interaction Problems—Part II: Implementation. *ASME 2009 28th International Conference on Ocean, Offshore and Arctic Engineering*, Honolulu, Hawaii, USA.

Liu, M.L. and Wu, J.F. (2012). Numerical Simulation for Ice-Truss Offshore Structure Interactions with Cohesive Zone Model. *21st IAHR International Symposium on Ice*, Dalian, China.

Lu, W., Løset, S. and Lubbard, R. (2012a). Simulating Ice-Sloping Structure Interactions with the Cohesive Element Method. *ASME 2012 31st International Conference on Ocean, Offshore and Arctic Engineering*, Honolulu, Hawaii, USA.

Lu, W., Lubbard, R., Løset S. and Hoyland, K. (2012b). Cohesive Zone Method Based Simulations of Ice Wedge Bending: A Comparative Study of Element Erosion, CEM, DEM and XFEM. *21st IAHR International Symposium on Ice*, Dalian, China.

Molinari, J.F., Gazonas, G., Raghupathy, R., Rusinek, A. and Zhou, F. (2007). The cohesive element approach to dynamic fragmentation: The question of energy convergence. *International Journal of Numerical Methods in Engineering*, Vol. 69, pp. 484-503.

Needleman, A. (1990). An analysis of decohesion along an imperfect interface. *International Journal of Fracture*, Vol. 42, pp. 21-40.

Papoulia, K.D., Sam C.H. and Vavasis, S.A. (2003). Time continuity in cohesive finite element modeling. *International Journal of Numerical Methods in Engineering*, Vol. 58, pp. 679-701.

Timco, G.W. and Weeks, W.F. (2010). A review of the engineering properties of sea ice. *Cold Regions Science and Technology*, Vol. 60, No. 2, pp. 107-129.